

importance for these catalysts, since the ions are presumed even more accessible when the clay has lost part of its crystalline structure. These samples also show the greatest percentage of Cr, as seen in Table I, which may also be a factor in the high conversions. In long-term experiments carried out to 20 cycles, the pillared clay (Cr-pb) is observed to be less stable.

Among the Cr(III)-containing catalysts, the pillared sample with Cr(III) presumed in the pillar (Cr*-pb) shows 100% conversion over 10 cycles, indicating high activity and high stability.

2. Selectivity. As received Bentolite L (b) is most selective for hexanes formation, as seen in Table V. Pillaring this (pb) produces a lower yield of hexane that decreases with time on stream. Cr*-pb does not produce significant amounts of products heavier than C₆; the major products from this catalyst are light hydrocarbons and coke. It appears, therefore, that a small amount (0.44 wt %) of chromium(III) in the pillars of pillared bentonite creates significant differences in catalytic hydrocracking.

3. Coking. The markedly higher yields of coke for the pillared clays follows a pattern previously reported by Occelli et al.²⁸ who observed greater yields of coke with PILC's than with H-Y zeolite during gas oil cracking. This was attributed in part to the open, two-dimensional structure of PILC's, which allows easier access for heavier hydrocarbons. Polycondensation reactions and coke formation is typical for Lewis acid sites abundant in PILC's.

During gas-oil conversion⁴ typical coking results are 7.8% C (coke/feed) for bentonite and 12.2% C for a pillared bentonite, i.e. approximately 65% higher. These values are in general agreement with our coke yields of 20% C for b and 38% C for pb. Adding Cr(III) ions to a bentonite drastically reduces the amount of coke formation, giving a value of only 4% C over four times as many cycles. Pillaring Cr-b increases the yield of coke to 12% C in 25 cycles. Significantly less coke (22% C) is observed when Cr(III) is added to the pillar (Cr*-pb) with respect to pb; this simultaneously increases the overall conversion as well. This is a further indication of significant catalytic effects associated

with the location of Cr(III) ions. Cr-b and Cr-pb display lower coke yields per cycle than pb and Cr*-pb.

The effects of the presence of zirconium(IV) ions in a pillar has also been studied by Occelli et al.⁸ By a comparison of APC and (Zr,Al)PC during propylene oligomerization at 480 °C, it was determined that (Zr,Al)PC produced less aromatics and more olefins and aliphatics and displayed less coke formation. APC had 17.2% C on the catalyst while (Zr,Al)PC had only 11.7% C. This was correlated to Lewis acidity. Coke yields for Cr(III)-doped PILC's may, therefore, also be a function of acidity, and we intend to explore this in future experiments.

Further experiments are now in progress to study different catalytic conditions, the role of the metal ion, and the feasibility of extending the use of these catalysts to heavier molecular weight hydrocarbons.²⁹

V. Conclusions

Diffuse reflectance and EPR spectroscopies indicate that chromium(III) ions in PILC's can exist in different environments depending on the methods of synthesis; two such important environments appear to be the micropore structure and in the pillar. Heating these catalysts in air converts the chromium to mixed oxidation states (e.g. III, V), but the major contributor appears to remain Cr(III). Catalytic activity for hydrocracking *n*-decane was strongly dependent on the location of the Cr(III) ions. Compared to a clay pillared with pure alumina, a PILC with Cr(III) apparently incorporated into the pillars was more active and more stable as a catalyst for hydrocracking *n*-decane.

Acknowledgment. The National Science Foundation, Grant No. CBT-8317876, supported this work. We thank Dr. Michael Seltzer of the Chemistry Department for suggestions concerning atomic absorption experiments, Southern Clay Products for providing bentonite clays, and Reheis Chemical Co. for providing the Chlorhydrol solution.

Registry No. Cr, 7440-47-3.

(28) Occelli, M. L.; Lester, J. E. *Ind. Eng. Chem. Prod. Res. Dev.* **1985**, *24*, 27.

(29) Skoularikis, N. D.; Carrado, K. A.; Kostapapas, A.; Suib, S. L.; Coughlin, R. W., manuscript in preparation.

Contribution from the Lehrstuhl für Theoretische Chemie, Ruhr-Universität Bochum, D-4630 Bochum, FRG

CEPA Calculations on Open-Shell Molecules. 7. Electronic Structure and Properties of HNS

Jan Wasilewski[†] and Volker Staemmler*

Received March 5, 1986

The HNS radical has been studied by quantum-chemical ab initio calculations in its lowest electronic states and in two isomeric forms, HNS and NSH. The calculations have been performed at the SCF level and with inclusion of electron correlation effects by means of the CEPA method. Equilibrium geometries, dipole moments, and force fields have been determined for the lowest electronic states as well as excitation energies, dissociation energies, ionization potentials, and electron affinities. HNS has a closed-shell ¹A' ground state with $R_{NH} = 1.03$ Å, $R_{NS} = 1.59$ Å, and $\vartheta_{HNS} = 107^\circ$. The lowest excited states are only 0.29 (³A'') and 0.96 eV (¹A'') above the ground state. NSH has also a ¹A' ground state which is 1.02 eV (23.4 kcal/mol) higher than the ¹A' ground state of HNS and has an equilibrium geometry with $R_{NS} = 1.52$ Å, $R_{SH} = 1.41$ Å, and $\vartheta_{NSH} = 109^\circ$. It seems that the barrier for thermal isomerization between these two isomers is not lower than the lowest dissociation energy (to H + NS). The bonding situation is discussed by using the results of population analyses.

1. Introduction

Sulfur imide (thionitroxyl), HNS, is an unknown molecule that so far has not been observed in isolated form. Only recently it was identified as a bridge ligand in an Fe₂ complex,¹ but its electronic structure in the complex is probably very different from

that of isolated HNS. Some thionitroso compounds of the form RNS have been observed as ligands in Fe₂ complexes as well (see ref 1 and references cited therein) or have been proposed as unstable organic compounds.²

[†] Permanent address: Institute of Physics, Nicholas Copernicus University, PL-87100 Torun, Poland.

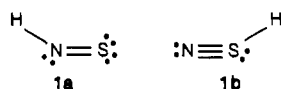
(1) Herberhold, M.; Bühlmeier, W. *Angew. Chem.* **1984**, *96*, 64; *Angew. Chem., Int. Ed. Engl.* **1984**, *23*, 80.
(2) Mehlhorn, A.; Sauer, J.; Fabian, J.; Mayer, R. *Phosphorus Sulfur* **1981**, *11*, 325.

Table I. Basis Sets Used for HNS and NSH

atom	Huzinaga's sp part ^a	basis symbol	additional functions on			no. of groups
			S	N	H	
D Bases (Double- ζ Type)						
S	10/6 \rightarrow 6/4	D11	d: 0.5	d: 0.8	p: 1.0	43
N	7/3 \rightarrow 4/2	D21	d: 0.95, 0.32	d: 0.8	p: 1.0	48
H	3 \rightarrow 2	D22	d: 0.95, 0.32	d: 1.8, 0.55	p: 1.0	53
		D32	d: 0.95, 0.32; f: 0.64	d: 1.8, 0.55	p: 1.0	60
T Bases (Triple- ζ Type)						
S	12/8 \rightarrow 8/5	T11	d: 0.5	d: 0.8	p: 1.0	53
N	9/5 \rightarrow 5/3	T21	d: 0.95, 0.32	d: 0.8	p: 1.0	58
H	5 \rightarrow 3	T22	d: 0.95, 0.32	d: 1.8, 0.55	p: 0.35	63
		T32	d: 0.95, 0.32; f: 0.64	d: 1.8, 0.55	p: 0.35	70
F Bases (D + Diffuse Functions)						
S } N } H }	like D	F32	s: 0.055; p: 0.06	s: 0.07; p: 0.09	p: 0.9	68
			d: 0.95, 0.32	d: 1.8, 0.55		
			f: 0.64			

^a References 19 and 20. 10/6 \rightarrow 6/4 means a 10s, 6p basis contracted to 6s and 4p groups; the steepest functions being always contracted together.

There are only very few ab initio calculations on HNS. Collins and Duke³ were the first authors to determine the equilibrium geometries of the two isomers HNS and NSH in their lowest closed-shell states. They found (SCF; basis set is single- ζ cores, double- ζ valence S and P, 1d on S, extra p on N, and p on H) that HNS is more stable than NSH by 25.6 kcal/mol and that the NS bond length is shorter by 0.08 Å in HNS than in NSH. This is surprising in view of the conventional chemical picture of a NS double bond in HNS (1a) and a triple bond in NSH (1b).



Mehlhorn et al.² performed ab initio (SCF, STO-3-21G basis set) and semiempirical (INDO, CNDO/S) calculations on HNS and found that the energy of the first excited $n\pi^*$ singlet state S_1 is only 0.97 eV above the closed-shell ground state S_0 (CNDO/S); the corresponding $n\pi^*$ triplet state T_1 is even below S_0 (SCF level). Recently, Hess et al.⁴ performed geometry optimizations at the SCF level with 6-31* basis sets for the lowest closed-shell states of HNS and NSH. Their results are similar to those of Collins and Duke;³ the main discrepancy is that their NS distance in NSH is markedly shorter than the one in ref 3. This is probably due to the inclusion of better d functions.⁴ Electron correlation effects have not been included in any of these calculations.

We conclude that the properties of HNS are still mostly unknown. Though it is probable that HNS is more stable than NSH, the energy difference between the two isomers is not well established and it is not known whether the isomerization barrier is small enough to allow for thermal isomerization. There are certainly low-lying electronically excited states, but the lowest excitation energies are uncertain and it might even be that the ground state of one of the two isomers is a triplet state.

Some small molecules that are isovalent with HNS are much better known. The FNS system has been studied quite intensely, both experimentally and by ab initio calculations.^{3,5-8} In this system, the NSF isomer is more stable than FNS. Its microwave and IR spectrum are well-known.⁹ The ground states of both isomers are closed-shell singlets. (See ref 8 for further references to experimental work.) Concerning the chemistry of NSF, we

refer to the review article by Glemser and Mews.¹⁰ Transition-metal thionitrosyl complexes of the form M-NS have also been reviewed recently.^{11,12}

Similarly, the HNO radical is quite well-known; there are in particular numerous ab initio studies of the potential energy surfaces and other properties of its lowest electronic states, for example in ref 13-15. The most complete study is that of Bruna,¹⁴ and we shall compare our results for the structure and properties of HNS frequently with Bruna's results on HNO. The high-resolution IR spectra of HNO and DNO in their closed-shell ground states have recently been studied by Johns et al.¹⁶

In this paper we present the results of an ab initio study of HNS and NSH in their lowest electronic states. The method of computation and the basis sets used are briefly described in section 2; section 3 contains the results for the geometrical structure of the lowest singlet and triplet states of the two isomers. In section 4 we present a prediction of excitation and dissociation energies, and in section 5 the chemical bonding in HNS and NSH is discussed.

2. Computational Methods

All the calculations have been performed by using the Bochum open-shell CEPA program.¹⁷ Correlation effects are included explicitly at the CI and CEPA levels. Each calculation consists of three different steps:

(a) A separate restricted (open-shell) SCF calculation is performed for each state under consideration.

(b) Inclusion of all configurations that are singly (S) and doubly (D) substituted with respect to the one-configuration SCF reference wave function is made. This yields a CI wave function with singles and doubles (CI-SD) or only a CI-D wave function if the singles are omitted.

(c) CEPA estimates are made of the effect of unlinked clusters of singles and doubles, CEPA-D and CEPA-SD, respectively. The formula given in ref 17 was used, and corresponds to the CEPA-2 recipe of Meyer.¹⁸ This formula yields reliable results only if the one-configuration reference is a good zeroth-order wave function. Furthermore, CEPA-SD is based on the assumption that the contribution of the singles is small. Both requirements are satisfied in the region of the minima of the two isomers—for all low-lying states—but they do not hold for large deviations from the respective minima, in particular not for the region of a possible isomerization barrier.

Basis sets of contracted Gaussian lobe functions have been used throughout. Orbital exponents and contraction coefficients for the s and

(3) Collins, M. P. S.; Duke, B. J. *J. Chem. Soc., Dalton Trans.* **1978**, 277.

(4) Hess, B. A.; Schaad, L. J.; Zahradnik, R., private communication, 1984.

(5) So, S. P.; Richards, W. G. *J. Chem. Soc., Faraday Trans. 2*, **1978**, 74, 1743.

(6) Seeger, R.; Seeger, U.; Bartetzko, R.; Gleiter, R. *Inorg. Chem.* **1982**, 21, 3473.

(7) Zirz, C.; Ahlrichs, R. *Inorg. Chem.* **1984**, 23, 26.

(8) Schaad, L. J.; Hess, B. A.; Čársky, P.; Zahradnik, R. *Inorg. Chem.* **1984**, 23, 2428.

(9) Cook, R. L.; Kirchoff, W. H. *J. Chem. Phys.* **1967**, 47, 4521.

(10) Glemser, O.; Mews, R. *Angew. Chem.* **1980**, 92, 904; *Angew. Chem., Int. Ed. Engl.* **1980**, 19, 883.

(11) Herberhold, M. *Nachr. Chem., Tech. Lab.* **1981**, 29, 365.

(12) Roesky, H. W.; Pandey, K. K. *Adv. Inorg. Chem. Radiochem.* **1983**, 26, 337.

(13) Nomura, O. *Int. J. Quantum Chem.* **1980**, 18, 143.

(14) Bruna, P. J. *Chem. Phys.* **1980**, 49, 39.

(15) Heibers, A.; Almlöf, J. *Chem. Phys. Lett.* **1982**, 85, 542.

(16) Johns, J. W. C.; McKellar, A. R. W.; Weinberger, E. *Can. J. Phys.* **1983**, 61, 1106.

(17) Staemmler, V.; Jaquet, R. *Theor. Chim. Acta* **1981**, 59, 487.

(18) Meyer, W. *Theor. Chim. Acta* **1974**, 35, 277.

Table II. SCF Energies, E_{SCF} , Valence-Shell Correlation Energies E_{CORR} , and Dipole Moments, $m = |\vec{m}|$, for the $^1A'$ (First Entry) and $^3A''$ (Second Entry) States of HNS^a

basis set	E_{SCF}	m_{SCF}	E_{CORR}			E_{CORR}		
			CI-D	CI-DS	m_{CI}	CEPA-D	CEPA-DS	m_{CEPA}
D11 ^b	-452.272 743	1.593	283.707	286.507	1.509	318.954	323.799	1.478
	-452.283 986	1.574	265.310	269.871	1.476	293.106	305.280	1.411
D21	-452.282 602	1.548	293.040	295.885	1.464	331.497	336.565	1.435
	-452.290 625	1.524	275.822	280.347	1.429	307.061	319.282	1.369
D22	-452.283 058	1.439	301.287	304.229	1.359	341.567	346.805	1.330
	-452.290 871	1.402	284.758	289.313	1.302	317.848	330.152	1.236
D32	-452.287 465	1.429	320.347	323.145	1.351	364.761	369.879	1.323
	-452.294 476	1.393	303.926	308.277	1.295	340.675	352.614	1.234
T11	-452.489 674	1.704	292.702	295.649	1.648	330.245	335.452	1.622
	-452.500 425	1.700	276.138	280.870	1.640	306.698	315.562	1.588
T21	-452.497 708	1.662	300.890	303.844	1.597	341.451	346.773	1.570
	-452.506 002	1.645	285.104	289.747	1.576	318.808	331.511	1.517
T22	-452.499 011	1.567	308.340	311.414	1.513	350.463	355.976	1.488
	-452.507 005	1.532	293.176	297.816	1.481	328.493	341.169	1.431
T32	-452.502 535	1.561	327.062	329.991	1.502	373.331	378.741	1.476
	-452.510 172	1.525	312.140	316.361	1.465	351.209	362.955	1.389
F32 ^c	-452.304 956	1.614	326.446	329.511	1.565	374.399	380.334	1.542
	-452.313 714	1.630	310.449	314.483	1.568	349.580	360.789	1.512

^a E_{SCF} in au, E_{CORR} in 10^{-3} au, m in D, distances in a_0 . 1 au = 27.2116 eV, 1 a_0 = 52.9177 pm. ^b Geometry (for bases D11–T32): for the $^1A'$ state, $R(\text{NS}) = 2.90$, $r(\text{NH}) = 1.92$, $\vartheta(\text{HNS}) = 105^\circ$; for the $^3A''$ state, $R = 3.05$, $r = 1.92$, $\vartheta = 110^\circ$. ^c Geometry: for the $^1A'$ state, $R = 3.01$, $r = 1.95$, $\vartheta = 107^\circ$; for the $^3A''$ state, $R = 3.03$, $r = 1.94$, $\vartheta = 114^\circ$.

p functions were taken from Huzinaga's tables;^{19,20} exponents for polarization functions and diffuse functions were chosen in close analogy to those optimized before in our group.^{21,22} Table I contains all the basis sets that we have used: In our shorthand notation for the basis sets, such as D21, the letter D means that we started from a double- ζ contraction of the s, p part, T stands for triple- ζ contraction, and F stands for double- ζ contraction plus diffuse functions. The two integers that follow indicate the number of full sets of polarization functions on S and N while on the hydrogen atom a full set of p functions was always used.

As a test of the basis sets and of the CI and CEPA variants, we have collected in Table II the SCF energies, the valence-shell correlation energies, and the dipole moments of the two lowest states, $^1A'$ and $^3A''$ of the HNS isomer. The geometries suggested by Mehlhorn et al.² were used for the D and T basis sets, for the F32 basis the geometries optimized with the D11 basis (see section 3) were taken. Though the absolute value of the SCF energy is lowered by ~ 0.2 au in going from the D and F basis sets to the T basis sets and though the valence-shell correlation energies are increased by $\sim 20\%$ between D11 and F32 bases, the calculated properties depend only slightly on the quality of the basis: The dipole moment becomes larger when the s,p part of the basis is improved, but smaller when more polarization functions are added. Correlation lowers its value in both states by ~ 0.1 D.

The singlet-triplet energy separation between $^1A'$ and $^3A''$ states is quite independent of the basis set: ~ -0.008 au (negative sign means $^3A''$ lower) at the SCF level and $\sim +0.010$ au with correlation included. This establishes the $^1A'$ state as the ground state of HNS, but confirms the results of Mehlhorn et al.² that at the SCF level the $^3A''$ state is lower than the $^1A'$ state; i.e., the ordering of the states is wrong. The differences of the four treatments of correlation effects are quite small; in the following we will generally only quote the CEPA-SD results, which in most cases are the most reliable ones.

3. PES Minima for the Two Isomers

For the two lowest states of the two isomers, i.e. the $^1A'$ and $^3A''$ states of HNS and NSH, we have determined the equilibrium geometries, harmonic force fields, and dipole moments at SCF and CEPA levels, but for economy reasons only the D11 basis set was used.

At SCF level about 80 points have been calculated in the vicinity of the minima of the three-dimensional surfaces depending on the three valence coordinates $R(\text{NS distance})$, $r(\text{NH or SH distance})$ and ϑ (valence angle). The calculations at the CEPA level were restricted to 20–30 points, which were distributed such that the

valence-shell correlation energy at intermediate points could be safely interpolated. Since the correlation energy in these regions of the surfaces is a slowly varying function of the coordinates, the accuracy of the interpolation was of the order of $(1-5) \times 10^{-6}$ au. The interpolation polynomial consisted of a full quadratic form in the variables R^{-1} , r^{-1} , and ϑ^{-1} and one third-order term $(Rr\vartheta)^{-1}$.

For the determination of the equilibrium geometries and the harmonic force fields we used conventional polynomial expansions in R , r , ϑ containing diagonal terms up to fifth order, all off-diagonal terms up to third order and one fourth-order term, namely R^2r^2 . The force field is expressed in dimensionless variables $\Delta R/R_0$, $\Delta r/r_0$, and $\Delta\vartheta$ instead of the classical variables ΔR , Δr , and $\Delta\vartheta$. In this approach, originally proposed by Mills,²³ the force field parameters have energy units, the conventional units like mdyn/Å are obtained by dividing by the appropriate equilibrium bond lengths (in a_0) and changing from atomic to metric units.

Table III contains some of our SCF results for the $^1A'$ ground states in comparison with results of the previous calculations,²⁻⁴ in particular the unpublished data of Hess et al.⁴ The results are quite similar; only the NS distance depends crucially on the basis set. Without d functions² it is much too long in both isomers; with one set of d functions on the S-atom³ HNS seems to be described fairly well, but NSH has still too large an NS distance. Our SCF force fields and vibration frequencies agree with those of Hess et al.⁴ fairly well.

Table IV contains our CEPA results for the same properties and for the rotational constants in a rigid-rotor approximation, calculated for the two lowest states, $^1A'$ and $^3A''$ of the two isomers. Comparison with Table III shows that electron correlation causes a rather large change in the NS distance of the $^1A'$ ground state of HNS. The change of $\sim 0.10a_0$ is accompanied by a large reduction of the force constant f_{RR} . The changes of most of the other properties are in the expected range.

The D11 basis set is certainly not large enough to allow for a very accurate calculation of force constants. We estimate that the errors in the calculated vibration frequencies are still in the order of 50–100 cm^{-1} . For the $^1A'$ state of HNS, ω_3 can be identified with the isolated NH stretching vibration (as the rather small off-diagonal force constants show); its value is comparable to that of isolated NH (3282 cm^{-1} in the $X^3\Sigma^-$ ground state²⁴)

(19) Huzinaga, S. *J. Chem. Phys.* **1965**, *42*, 1293.

(20) Huzinaga, S. "Approximate Atomic Functions I and II"; University of Alberta: Edmonton, AB, Canada, 1971.

(21) Ahlrichs, R.; Driessler, F.; Lischka, H.; Staemmler, V.; Kutzelnigg, W. *J. Chem. Phys.* **1975**, *62*, 1235.

(22) Ahlrichs, R.; Keil, F.; Lischka, H.; Kutzelnigg, W.; Staemmler, V. *J. Chem. Phys.* **1975**, *63*, 455.

(23) Mills, I. M. *Theoretical Chemistry*; Specialist Periodical Report; The Chemical Society: London, 1974; Vol. 1, p 110.

(24) Huber, K. P.; Herzberg, G. *Molecular Spectra and Molecular Structure. IV. Constants of Diatomic Molecules*; Van Nostrand Reinhold: New York, 1979.

Table III. SCF Results for Equilibrium Geometries, Force Fields and Harmonic Vibration Frequencies for HNS and NSH in Their $^1A'$ Ground States

	HNS				NSH		
	<i>a</i>	<i>b</i>	<i>c</i>	<i>d</i>	<i>a</i>	<i>b</i>	<i>c</i>
geometry ^e							
R_c	2.927	2.908	2.93	3.06	2.886	2.857	3.08
r_c	1.922	1.909	1.90		2.596	2.559	2.56
ϑ_c	110	111	100		107	108	104
force fields ^f							
f_{RR}	5.0229	4.9946			3.7740	3.9295	
f_{rr}	1.7081	1.7398			1.5872	1.7078	
$f_{\vartheta\vartheta}$	0.2282	0.2278			0.3108	0.3197	
f_{Rr}	0.00097	-0.0071			0.3391	0.2687	
$f_{R\vartheta}$	0.2082	0.1874			0.2229	0.2261	
$f_{r\vartheta}$	0.0078	0.0051			-0.0420	-0.0373	
harmonic vibration frequencies ^g							
ω_1	1231 (0.077)	1281 (0.138)			1072 (0.152)	1077 (0.054)	
ω_2	1338 (1.0)	1355 (1.0)			1169 (0.018)	1234 (0.201)	
ω_3	3607 (0.333)	3665 (0.130)			2575 (1.0)	2658 (1.0)	

^aThis work, D11 basis set. ^bHess et al.,⁴ SCF gradient calculations, 6-31* basis. ^cCollins and Duke,³ SCF, the basis corresponds to a D10 basis in the designation of Table I. ^dMehlhorn et al.,² SCF, 3-21 basis. ^e*R* and *r* in a_0 . ^fForce constants in energy units (see text). ^g ω in cm^{-1} . Values in parentheses are relative IR intensities.

Table IV. CEPA Results for Equilibrium Geometries and Spectroscopic Properties of the Lowest $^1A'$ and $^3A''$ States of HNS and NSH^a

	HNS		NSH	
	$^1A'$	$^3A''$	$^1A'$	$^3A''$
R_c ^b	3.028	2.932	2.878	3.263
r_c	1.957	1.922	2.663	2.544
ϑ_c	107.1	125.1	109.4	94.8
f_{RR} ^c	3.9494	3.7181	4.0251	2.0291
f_{rr}	1.5279	1.7866	1.1574	1.7449
$f_{\vartheta\vartheta}$	0.2208	0.1136	0.2809	0.1709
f_{Rr}	0.0177	-0.4176	0.3715	0.0383
$f_{R\vartheta}$	0.2298	0.2675	0.1945	0.0959
$f_{r\vartheta}$	0.0043	0.0405	-0.0355	-0.0016
ω_1 ^d	1045 (0.011)	817	1086 (0.055)	703
ω_2	1286 (1.0)	1106	1110 (0.018)	877
ω_3	3349 (0.082)	3718	2147 (1.0)	2753
A^e	18.9	27.7	10.1	9.65
B	0.62	0.64	0.72	0.57
C	0.60	0.63	0.67	0.54

^aThis work, CEPA-D, D11 basis set. ^bDistances in a_0 . ^cIn energy units, see text. ^dIn cm^{-1} ; in parentheses are given relative IR intensities. ^eRotational constants; rigid rotor approximation.

and to that of the HNS ligand of Herberhold et al. (3365 cm^{-1}).¹ The NS stretching and the bending vibration are strongly mixed.

In Figure 1 we have represented the two isomers in the two lowest states in their principal inertial frame. The components of the dipole moments in Cartesian coordinates with *x* perpendicular to the molecular plane and *z* along the NS axis are as follows (all values in D; F32 basis set; CEPA-SD): 0, 1.542, -0.023 (HNS, $^1A'$); 0, 1.511, -0.056 (HNS, $^3A''$); 0, 0.760, 2.751 (NSH, $^1A'$); 0, 1.103, 1.457 (NSH, $^3A''$).

4. Excitation and Dissociation Energies

For a more precise prediction of (adiabatic) excitation energies, ionization potentials, and electron affinities, we have performed a series of calculations with basis F32. This basis contains sufficient polarization functions to account for ~85% of the valence-shell correlation energy and also diffuse functions for a satisfactory description of diffuse orbitals in higher excited states and in the negative ions. For the lowest $^1A'$ and $^3A''$ states of HNS and NSH we took the geometries optimized at the CEPA level with the D11 basis set (compare with section 3); for the other states the geometry optimization was performed at the SCF level, D11 basis. The results are collected in Table V; a correlation diagram is given in Figure 2.

On the SCF level, the $^3A''$ state is lower than the $^1A'$ state both for HNS and for NSH and also for all basis sets used. Inclusion of electron correlation reverses the order of the two states

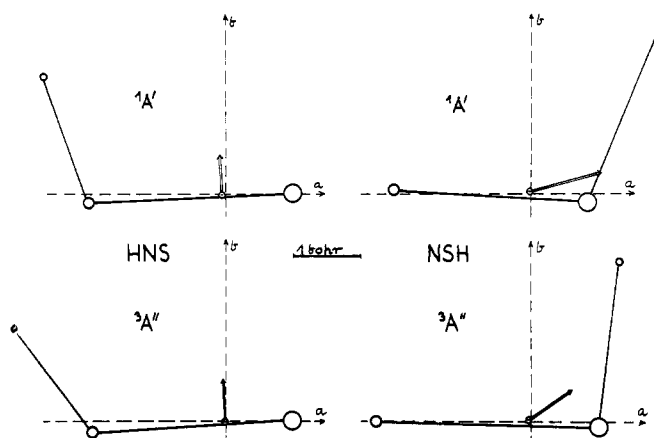


Figure 1. HNS and NSH isomers in the $^1A'$ and $^3A''$ states presented in the principal inertial frame (equilibrium geometries). The dipole moment vectors start from the center of negative charge. CEPA-SD, F32 basis set, was used.

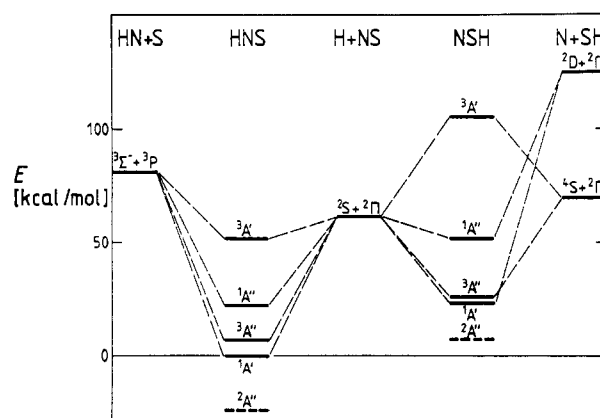


Figure 2. Correlation diagram for the lowest states of HNS and NSH vs. the possible dissociation products. F32 basis set, CEPA-SD, was used. The dashed levels indicate the negative ions HNS^- and NSH^- , respectively.

since the valence-shell correlation energy is larger for the closed-shell $^1A'$ state than for $^3A''$, which contains two unpaired electrons (stabilization of ~0.5 eV for HNS and ~0.9 eV for NSH). The $^1A'$ - $^3A''$ energy separation is very small (0.29 eV in HNS, 0.12 eV in NSH), and also the next excited states ($^1A''$ and $^3A'$ for HNS and $^1A'$ for NSH) are still below the lowest dissociation limit to $\text{H}(^2S) + \text{NS}(^2\Pi)$. We have checked by a

Table V. Energies of HNS Isomers and Their Dissociation Products

system	state	geometry ^a			energy ^b		ΔE^c
		R	r	ϑ	SCF	CEPA-SD	
HNS	1 ¹ A'	3.01	1.95	107	-452.304 956	-452.685 290	0.00
	1 ³ A''	3.03	1.94	114	-452.313 714	-452.674 503	0.29
	1 ¹ A''	3.15	1.93	106	-452.297 727	-452.649 948	0.96
	1 ³ A'	3.53	1.92	103	-452.263 629	-452.601 815	2.27
NSH	1 ¹ A'	2.88	2.66	109	-452.276 738	-452.647 972	0.00
	1 ³ A''	3.25	2.54	95	-452.303 108	-452.643 472	0.12
	1 ¹ A''	3.10	2.54	98	-452.249 484	-452.601 711	1.26
	1 ³ A'	3.30	2.58	109	-452.176 759	-452.517 032	3.56
HNS ⁺	2 ² A'	2.76	1.93	130	-452.003 393	-452.358 796	8.88
HNS ⁻	2 ² A''	3.25	1.97	103	-452.340 462	-452.723 286	1.03
NSH ⁺	2 ² A'	2.89	2.65	97	-451.959 698	-452.309 685	9.21
NSH ⁻	2 ² A''	3.08	2.76	112	-452.293 041	-452.673 456	0.69
H	2 ² S				-0.5	-0.5	
N	4 ⁴ S				-54.341 607	-54.453 ^d	
N ⁺	3 ³ P				-53.829 419	-53.921 297	
N ⁻	3 ³ P				-54.265 038	-54.414 874	
S	3 ³ P				-397.346 500	-397.493 382	
S ⁺	4 ⁴ S				-397.008 375	-397.116 ^d	
S ⁻	2 ² P				-397.380 323	-397.556 171	
NH	3 ³ Σ^-		1.958		-54.915 331	-55.062 103	
SH	2 ² Π		2.550		-397.939 973	-398.120 381	
SH ⁺	3 ³ Σ^-		2.550		-397.597 650	-397.745 981	
NS	2 ² Π	2.825			-451.727 927	-452.086 642	
NS ⁺	1 ¹ Σ^+	2.721			-451.410 906	-451.766 613	
NS ⁻	3 ³ Σ^-	2.825			-451.757 342	-452.115 037	

^aAll distances in a_0 . $R = R_{NS}$, $r = R_{XH}$. Geometries are optimized with basis D11 on the CEPA level for the 1¹A' and 1³A'' states of HNS and NSH and on the SCF level for the other states. For diatomic fragments experimental distances were used.²⁴ ^bAll energies in atomic units; basis F32. ^cIn eV; CEPA-SD, relative to the 1¹A' ground state of the same isomer. ^dEstimated since our CEPA program cannot treat quartet states. It is assumed that CEPA basis F32 covers 87% of the known valence-shell correlation energies for N(⁴S) and S(³4S) as it does for N(³P) and S(³P).

series of small CI calculations that the states included in Table V are indeed the lowest states of HNS and NSH. However, in the vicinity of the fourth (1³A') state of NSH there might be two more states (2¹A', 2³A').

The situation is rather similar to that in the HNO system. According to Bruna,¹⁴ the HNO isomer has a closed-shell singlet ground state, 1¹A', and a pair of low-lying excited A'' states with excitation energies of 1–2 eV, which can be characterized by a 7a' → 2a'' excitation. In NOH, on the other hand, the 1³A'' is below the 1¹A' state even after CI.¹⁴ With this exception, the number and relative energetic order of the low-lying states in HNO agree with our results for HNS, but all the energy separations are much smaller in HNS than in HNO. The fact that the closed-shell 1¹A' ground state and two reactive open-shell states are within 1 eV in HNS is probably the reason that this molecule has not been observed so far though it is stable against dissociation in all these states (see next section).

From the data of Table V it is seen that the HNS isomer in its lowest 1¹A' state is 17.7 kcal/mol (SCF level) or 23.4 kcal/mol (CEPA-SD) lower in energy than NSH in the 1¹A' ground state. The SCF value of Collins and Duke³ of 25.6 kcal/mol is substantially higher than our SCF value, probably since the d functions play a more important role in the chemical bonding of the NSH isomer (see section 5). In the HNO system, Bruna¹⁴ found the 1¹A' state of HNO to be 44.5 kcal/mol more stable than the 1¹A' state of NOH (which is not the ground state of NOH). This is again an indication of smaller energy differences in HNS as compared to HNO.

We have also included results for the ground states of the positive and negative ions of the two isomers of HNS in Table V. The (adiabatic) first ionization energies are rather low: our calculations, CEPA-SD, F32 basis, yield 8.88 eV for HNS and 9.21 eV for NSH. We estimate that the true values should be ~0.2 eV larger with an error of ~0.1 eV. These low values indicate that the highest occupied MOs are nonbonding or even antibonding, in agreement with the strong bond contraction upon ionization in HNS (see also section 5).

The electron affinities are in the order of 1 eV (1.03 eV for HNS, 0.69 eV for NSH), which is in reasonable agreement with

Table VI. Heats of Formation and Bond Energies of HNS Isomers in Their 1¹A' Ground States^a

system	ΔH_f°				
	exptl ^b	exptl ^c	SCF ^d	CEPA-SD ^d	extrap ^e
H + N + S	229.8 ± 0.2	0	0	0	0
H + NS	114 ± 25	-115 ± 25	-25.0	-88.0	-112 ± 5
HN + S	156 ± 4	-74 ± 4	-46.3	-68.5	-72 ± 2
HS + N	145.7 ± 1.2	-84.1 ± 1.2	-58.7	-79.7	-84 ± 2
HNS(1 ¹ A')			-73.3	-149.9	-175 ± 7
NSH(1 ¹ A')			-55.6	-126.5	-153 ± 7
bond	D_e			D_0	
		SCF ^d	CEPA-SD ^d	extrap ^e	
	H-NS	48.3	61.9	64 ± 2	
	HN-S	27.1	81.5	103 ± 5	
	N(⁴ S)-SH	-3.1	46.8	69 ± 5	
N(² D)-SH ^f	51.7	101.6	124 ± 5		
NS-H	30.6	38.5	40 ± 2		

^aAll entries in kcal/mol; 1 au = 627.5 kcal/mol. ^bReference 25. ^cExperimental values, but relative to H + N + S. ^dThis work; basis F32; pure electronic energies. ^eExtrapolated (see text). ^fOur calculation for N(⁴S)-SH, plus experimental excitation energy N(⁴S) → N(²D).²⁶ The lowest dissociation channel, NSH(1¹A') → N(⁴S) + SH(² Π) is of course spin forbidden.

the values for other systems containing partly filled antibonding orbitals.

From the total energies of the HNS isomers and their various dissociation products, which are also included in Table V, thermochemical data can be estimated. Table VI contains the calculated heats of formation and dissociation energies for the lowest dissociation channels of the 1¹A' states of the two isomers in comparison with experimental heats of formation.²⁵ The ΔH_f°

(25) Chase, M. W., Jr.; Curnutt, J. L.; Downey, J. R.; McDonald, R. A.; Syverud, A. N.; Valenzuela, E. A. *J. Phys. Chem. Ref. Data* 1982, 11, 695.

Table VII. Mulliken Population Analysis for HNS and NSH: First Entry, D21 Basis; Second Entry, F32 Basis

isomer	state	atom	population				net charge
			s	p	d	f	
HNS ^a	¹ A'	S	5.84	9.82	0.12	0.02	+0.22
			5.97	9.83	0.12		+0.06
		N	3.78	3.62	0.04		-0.44
			3.69	3.52	0.05		-0.26
			0.74	0.04			+0.22
H	0.76	0.05		+0.19			
HNS ^b	³ A''	S	5.83	9.72	0.13	0.02	+0.33
			5.98	9.73	0.14		+0.12
		N	3.71	3.81	0.03		-0.55
			3.58	3.71	0.04		-0.33
			0.73	0.04			+0.23
H	0.75	0.05		+0.20			
NSH ^c	¹ A'	S	5.73	9.62	0.25	0.03	+0.41
			5.84	9.62	0.26		+0.26
		N	3.92	3.51	0.04		-0.47
			3.88	3.40	0.05		-0.33
			0.92	0.02			+0.06
H	0.91	0.02		+0.07			
NSH ^d	³ A''	S	5.79	10.01	0.12	0.01	+0.07
			5.89	10.03	0.12		-0.05
		N	3.95	3.25	0.02		-0.22
			3.88	3.17	0.03		-0.09
			0.83	0.02			+0.15
H	0.84	0.03		+0.14			
NS ^e	² II	S	5.81	9.61	0.14	0.02	+0.36
			5.94	9.72	0.15		+0.17
		N	3.91	3.40	0.05		-0.36
			3.85	3.27	0.05		-0.17

^a Geometry $R/r/\vartheta$: 3.028/1.957/107.1. R and r in a_0 ; ϑ in deg. ^b Geometry $R/r/\vartheta$: 2.932/1.922/125.1. ^c Geometry $R/r/\vartheta$: 2.878/2.663/109.4. ^d Geometry $R/r/\vartheta$: 3.263/2.544/94.8. ^e $R = 2.825a_0$.

value for NS is still quite uncertain. In the correlation diagram of Figure 2 the lowest dissociation channels are also included.

Two comments concerning the accuracy of our results are necessary:

(a) We have calculated pure electronic energies; i.e., our dissociation energies represent D_e and not D_0 values, and the same is true for the heats of formation. In order to allow for a fair comparison with experiment we have to reduce our results by the corresponding zero point energies, which are estimated to be (in kcal/mol) 4.6 (HN²⁴), 3.8 (HS²⁴), 1.7 (NS²⁴), 8.1 (HNS, ¹A', from Table IV), and 6.2 (NSH, ¹A', from Table IV).

(b) The basis F32 accounts for only 80–85% of the valence-shell correlation energies. Since a large part of the binding energy is due to electron correlation (which can be easily seen by comparing our SCF and CEPA-SD results), the calculated binding energies and heats of formation are considerably too low. The error is particularly large if a multiple bond, as e.g. in NS, is broken. We have performed separate calculations for H₂ and N₂, with basis F32 yielding the following binding energies (in kcal/mol): for H₂, 83.2 (SCF), 105.3 (CEPA-SD), 109.4 (experimental D_e value²⁴); for N₂, 118.2 (SCF), 193.0 (CEPA-SD), 228.4 (experimental²⁴). From these figures one can expect that our binding energies for the HN and HS single bonds are 6–10 kcal/mol too low; for the NS double bond they are 20–30 kcal/mol too low.

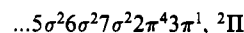
Combining these two effects, we arrive at the "extrapolated" values for ΔH_f° and D_e given in Table VI.

Finally, we have tried to find a transition state for the isomerization of HNS to NSH in the ¹A' state. Since neither the SCF nor the CEPA method is appropriate for regions on the potential surface that cannot be well described with a single-configuration reference, we have also applied small-valence CI calculations starting from different sets of orbitals. All these attempts failed. We could not find a transition state with an energy below the lowest dissociation channel H+NS. Though

these calculations are only of qualitative nature, we think that the conclusion is correct. This is supported by two arguments: First, in his MRD-CI calculations on the HNO system Bruna¹⁴ found a transition state with an isomerization barrier higher than the smallest dissociation energy. Secondly, since the bonding of H to NS involves an antibonding π orbital on NS with a nodal surface intersecting the NS axis (see section 5), a stable "triangular" NHS structure seems improbable.

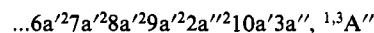
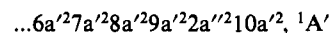
5. The Chemical Bond in the HNS Isomers

The origin of the chemical bonding in HNS is most easily understood, if one starts from the electronic structure of the NS radical in its ²II ground state. The occupation of the valence orbitals is given by



with the doubly degenerate antibonding 3π orbital singly occupied. This orbital has a nodal surface intersecting the NS axis in addition to the π -type nodal plane containing the molecular axis. The orbital is strongly polarized towards the N atom; a population analysis (F32 basis) shows that N AOs contribute ~66% to it. The net charge on N is -0.17, and the dipole moment is 1.59 D with the negative end on the N atom (SCF, F32 basis).

If an hydrogen atom is approaching the NS radical, the symmetry is reduced to C_s . The in-plane (a') component of the 3π orbital can be combined with the 1s AO of H to a bonding ($10a'$) and an antibonding a' orbital; the out-of-plane component is unaffected and has a'' symmetry. The electronic structure of the lowest states of HNS can therefore be characterized by the MO scheme



Since 3π is mainly located on the N atom, formation of a bonding $10a'$ orbital is most favorable if the hydrogen is approaching toward the N atom and less favorable for the approach

(26) Moore, C. E. "Atomic energy levels"; *Natl. Stand. Ref. Data Ser. (U.S. Natl. Bur. Stand.)* 1971.

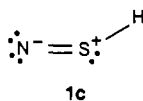
toward S. No bonding orbital can be formed if H approaches between N and S, i.e. along the nodal surface of the NS-antibonding 3π orbital. The $10a'$ orbital is NH bonding (or SH bonding) but partially NS antibonding, since it is constructed from the NS-antibonding 3π orbital.

In the $^1A'$ ground states of both isomers the NS-antibonding $10a'$ orbital is doubly occupied. One therefore expects a lengthening of the NS bond as compared to isolated NS in which the antibonding 3π orbital is only singly occupied. The optimized geometries in Table V show that this is indeed the case for HNS and to a smaller extent for NSH. As a population analysis (see below) reveals, in NSH some charge reorganization has to take place before bonding.

For the two A'' states we expect a higher energy since the bonding $10a'$ orbital is only singly occupied. Since both singly occupied orbitals are NS antibonding we also expect a bond lengthening compared to NS. Table V shows that these predictions are correct; in most cases the NS bond length is even larger than in the $^1A'$ states, probably because $3a''$ is more strongly antibonding than $10a'$. The energetic splitting of the two states is governed by the exchange integral ($10a'3a''/3a''10a'$) as discussed by Bruna for HNO.¹⁴

Table VII contains results of a Mulliken population analysis for the two lowest states of both isomers, performed for the basis sets D21 and F32. Obviously, the net charges on N and S are considerably reduced if the basis is improved, but the main conclusions are independent of the basis set.

In HNS (both states) the N atom carries substantial negative charge, which comes mainly from H and to a smaller extent from S (F32 basis). This is in agreement with the conventional electronegativities of the atoms. The population of the d AOs on S is small, d AOs act merely as polarization functions. The s and p populations on N correspond to a $sp^{2.08}$ hybridization, while in isolated NS it is $sp^{1.77}$. All this can be interpreted as an ordinary NS double bond as represented by **1a**. On the other hand, in the $^1A'$ ground state of NSH the N atom is even slightly more negative, but the positive charge is predominantly located on S, H being almost neutral. In addition, the d AO population on S is much larger than in all other states (0.26 as compared to 0.13 elsewhere), and the hybridization of the N atom is $sp^{1.81}$, i.e. close to that in NS. The bonding situation in the $^1A'$ states of NSH can therefore be described by the limiting structures of a triple bond (**1b**) and an ionic bond (**1c**), i.e. it is a semipolar triple bond.



Contour plots of the four highest occupied MOs of HNS in the $^1A''$ state are given in Figure 3.

The size and orientation of the dipole moment (compare with Figure 1) agrees well with this interpretation and with the net charges of Table VII. The NS bond length (3.01 a_0 in HNS and only 2.88 a_0 in NSH) also supports our interpretation.

The chemical bond in the ground states of the two isomers of HNS is very similar to that found and analyzed in detail by Wallmeier and Kutzelnigg²⁷ in XO compounds (X = N, P, S). The pair H_2POH and H_3PO closely resembles the pair HNS and NSH; there is a PO single bond with a d population on P of 0.15 in H_2POH , but a semipolar PO double bond with a d population of 0.30 in H_3PO . Similarly, HSOH has a SO single bond, d population of 0.11, while H_2SO has a semipolar double bond with a d population of 0.26.²⁷ In particular, these latter values are almost identical with those given in Table VII.

The bonding situation in the closed-shell $^1A'$ ground state of the FNS system, which has been discussed in some detail by Seeger et al.⁶ and by Zirz and Ahlrichs⁷ is quite different from that in HNS. The NSF isomer is about 21 kcal/mol more stable than FNS (ref 6; best basis together with the inclusion of correlation effects). The reason is that the high electronegativity of the F

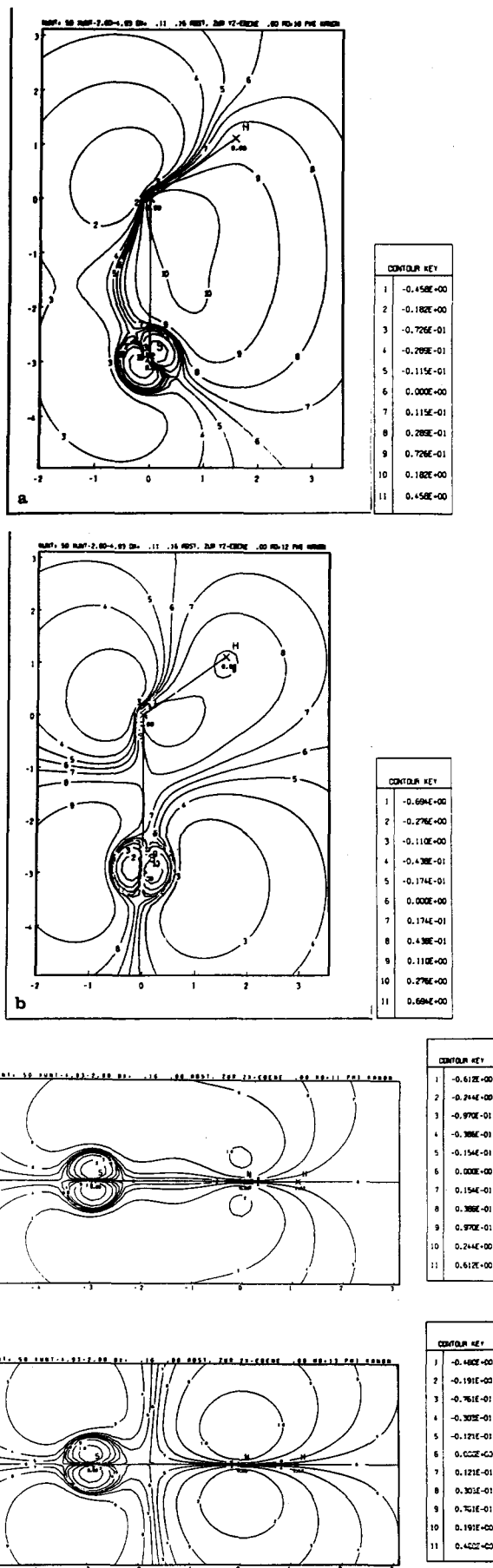


Figure 3. Contour plots of the four highest occupied MOs of the $^1A''$ state of HNS: (a) $9a'$, (b) $10a'$, (c) $2a''$, (d) $3a''$.

(27) Wallmeier, H.; Kutzelnigg, W. *J. Am. Chem. Soc.* **1979**, *101*, 2804.

atom enables a strong polar SF bond while the FN bond is predominantly covalent. Thus, the approach of the F atom toward the S end of NS is preferred, and both the NS and the SF bonds are strongly semipolar in NSF.⁷ Again, this is reflected in the importance of d functions on S. Seeger et al.⁶ found that without d AOs FNS and NSF have approximately the same stability and that the d population on S is very high in NSF (0.375 as compared to our value of 0.26 in NSH), but small in FNS (0.117 while we obtained 0.12 in HNS).

6. Conclusions

The main results of our study of the properties of the HNS radical can be summarized as follows:

(1) HNS and NSH are two independent isomeric species; there is no low-lying barrier that can allow for a thermal isomerization. In their respective ¹A' ground states HNS is 23.4 kcal/mol more stable than NSH.

(2) Though both isomers have closed-shell ¹A' ground states, they have to be considered as highly reactive radicals since they possess several low-lying electronically excited states. The lowest

excitation energies are much lower than in the isovalent molecules HNO and (probably) NSF.

(3) The chemical bond in the ground states of the two isomers can be characterized as a conventional NS double bond in HNS and a semipolar triple bond in NSH. The latter is similar to the semipolar bonds in H₂SO, H₃PO, and NSF.

(4) Reliable results for most properties (relative stabilities, excitation energies, geometries) require good basis sets (including d AOs at least on S) and the inclusion of correlation effects.

Acknowledgment. We thank the Alexander von Humboldt-Foundation and the Deutsche Forschungsgemeinschaft who made the stay of Jan Wasilewski in Bochum possible. All calculations were performed on the Interdata 8/32 minicomputer at the Lehrstuhl für Theoretische Chemie in Bochum, which was sponsored by the Deutsche Forschungsgemeinschaft. We also thank Prof. Hess (Nashville, TN) for providing us with his unpublished results on HNS. The contour plots of Figure 3 are due to U. Fleischer (Bochum).

Registry No. HNS, 14501-19-0; NSH, 36529-67-6.

Contribution from the Department of Chemistry,
University of Leuven, Celestijnenlaan 200F, 3030 Leuven, Belgium

Multiplet Theory of Transition-Metal Ions

L. G. Vanquickenborne,* P. Hoet, and K. Pierloot

Received April 7, 1986

For a number of ions of the 3d-transition-metal series (V, Cr, Mn, Fe, Co), the experimental excitation energies of the dd bands have been analyzed on the basis of the quantum-mechanical virial theorem and the Hellmann-Feynman theorem. It is shown that the energy sequence of the different 3d^q multiplets is determined predominantly by the relative value of the electron-nuclear attraction energies. This result is in agreement with an earlier Hartree-Fock study; it contrasts with the conventional multiplet theory of Slater-Condon-Shortley, where the relative energy of the different (*L,S*) terms is explained in terms of differences in d-d repulsion energy. Certain implications for ligand field theory are briefly discussed.

Introduction

In transition-metal ions, any *nd*^q configuration (1 < *q* < 10) gives rise to a number of (*L,S*) multiplets, whose energy separation is described qualitatively by the well-known Slater-Condon-Shortley (SCS) theory.^{1,2} This is essentially a first-order perturbation approach, starting off from a presupposed set of orbitals, which are occupied in a variety of ways. In the SCS theory, the energy difference between two multiplets stems entirely from the difference in the corresponding *open-shell repulsions*: different ways of having the *nd* shell occupied by *q* electrons correspond to different average interelectronic distances, and hence different interelectronic repulsions. If we denote the total electronic energy by *E*, the expectation value of the kinetic energy by *T*, the nuclear attraction by *L*, and the repulsion by *C*, we have

$$E = T + L + C = T + V = H + C \quad (1)$$

and the conventional SCS theory describes the energy difference between two *nd*^q multiplets as

$$\Delta E = \Delta C = \Delta C_0 \quad (2)$$

where *C*₀ refers to the open-shell (d-d) repulsion energy and

$$\Delta T = \Delta L = \Delta H = 0 \quad (3)$$

If the explicit analytical expression of the radial functions (the orbital "shape") is not known explicitly, the $\Delta E = \Delta C$ values are described by means of semiempirical parameters, viz. the Sla-

ter-Condon *F_k* integrals or alternatively the Racah parameters *B* and *C*.

SCS theory is able to account for Hund's rules: more specifically, it predicts that the highest spin state is the ground state, because the highest spin state is calculated with the lowest interelectronic repulsion. In a similar way, the spin-pairing energy,^{3,4} i.e. the energy required to turn two spins from parallel to antiparallel, can be shown to be a positive quantity:

$$E(S-1) - E(S) = 2SD \quad (4)$$

$$D = \frac{7}{6}K_{av} \quad (5)$$

where *E*(*S*) is the weighted mean energy of the *d*^q multiplets characterized by *S* spin quantum number and where *D*, the spin-pairing parameter, is positive, since it is proportional to *K*_{av}, the average exchange integral of the *d*^q system. *D* is a simple function of the relevant *F_k* integrals, and eq 4 shows in a very compact way how conventional multiplet theory ascribes spin pairing to an increased interelectronic repulsion. The spin-pairing energy is an important parameter in transition-metal chemistry, since its magnitude (with respect to 10*Dq*) determines if a given complex will be of high-spin or low-spin type.^{2,5}

Application of Two Quantum-Mechanical Theorems

A. The Virial Theorem. Although conventional SCS multiplet theory is both simple and successful, it obviously violates the virial

(1) Slater, J. C. *Quantum Theory of Atomic Structure*; McGraw-Hill: New York, 1960; Vols. I, II.
(2) Ballhausen, C. J. *Introduction to Ligand Field Theory*; McGraw-Hill: New York, 1962.

(3) Slater, J. C. *Phys. Rev.* **1968**, *165*, 655.

(4) Jørgensen, C. K. *Atomic Spectra and Chemical Bonding in Complexes*; Pergamon: Oxford, 1962.

(5) Lever, A. B. P. *Inorganic Electronic Spectroscopy*, 2nd ed.; Elsevier: Amsterdam, 1984.